



Hydraulic performance of bottom intake velocity caps using PIV and OpenFOAM methods

Zahra Hajebi¹ · Mahmood Rahmani Firozjaei¹ · Seyed Taghi Omid Naeeni¹ · Hassan Akbari²

Received: 20 October 2023 / Accepted: 25 December 2023 / Published online: 7 February 2024
© The Author(s) 2024

Abstract

The objective of this investigation is to obtain a more profound understanding of the effective parameters of the velocity caps for bottom intake systems, utilizing particle image velocimetry (PIV) and OpenFOAM. Observations indicate a higher probability of surface vortex formation in square types compared to circular ones, with the vortex being formed downstream of the caps. Additionally, the flow pattern reveals that the flow whirls in a more favorable path into the circular caps as opposed to the square ones. Through both experimental and numerical comparisons of three shapes (rhombus, square, and circle), it becomes evident that the circular type outperforms the other types in terms of discharges through the intake, showing an improvement of about 8%. The results indicate that flow depth and height of the velocity caps are positively effective parameters for the flow rate, with respective influences of 90% and 30%. In contrast, the interaction between the flow and caps intensifies with an increase in the distance of the intake opening from the bed, which plays a negative influence on the flow rate. Enhancing the number of blades in caps proves to be the optimal approach for generating a smoother flow with minimal impact on the flow rate. Numerical simulations show a 50% reduction in cap height leads to a significant 33% decrease in flow rate. Additionally, rotating the square cap by 45° into a rhombus aligned with the flow direction results in a 7% discharge flow rate increase.

Keywords Particle image velocimetry · OpenFOAM · Seawater intake · Bottom intake · Velocity cap

List of symbols

A	Area of velocity cap (m^2)
B	Main channel width (m)
C_d	Discharge coefficient through the intake (m^3/s)
D	Diameter of the orifice (m)
h	Height of the velocity cap (m)
H	Head of water above the centerline of the orifice (m)
Fr	Froude number in the main channel

N	Number of blades
Q_{intake}	Discharge
Q	Discharge in the main channel (m^3/s)
Y_m	Water depth in main channel (m)
w	The distance of opening of intake from the channel bed (m)

Introduction

Unfortunately, the lack of freshwater resources is increasing due to climate change and urbanization development. As a result, different countries are looking to use sea water, as a huge water reservoir. Using sea water and removing its salt and mineral components is one of the solutions that humans have utilized to overcome water shortages. However, an important factor for all types is that they require a continuous discharge of water to enhance their functions (Aghazadeh and Attarnejad 2020a, b). Coastal facilities such as seawater desalination technology are increasing as supplementary or even main water sources for various countries, and they require a continuous discharge of water to

✉ Mahmood Rahmani Firozjaei
Mrahmanif69@gmail.com; Mrahmanif69@ut.ac.ir

Zahra Hajebi
Zahrahajebi@ut.ac.ir

Seyed Taghi Omid Naeeni
Stnaeeni@ut.ac.ir

Hassan Akbari
Akbari.h@modares.ac.ir

¹ School of Civil Engineering, College of Engineering, University of Tehran, Tehran, Iran

² School of Civil and Environmental Engineering, Tarbiat Modares University, Tehran, Iran

manufacture their functions. One of the most suitable intake structures to divert flow from the sea is bottom intake structure. The systems are usually consisting of pipelines located on the seabed and velocity caps.

Greenlee et al. (2009) stated that a bottom intake structure is a better choice compared with other seawater intake methods due to high-water supply capacity. Missimer et al. (2013) stated that the depth of water intake is a very important factor. So, the water intake structure is placed far from the coastal area in order to reduce the surface pollution and decrease the effect of waves. One of the environmental effects of seawater intake is the threat to marine life. Doni (2018) stated that one of the intake structures that can be used for this purpose is the so-called velocity cap. Also, the specific geometry of the velocity cap curbs the formation of a surface vortex and protects them from bed sediments taken in. Lee and Wahab (2019) conducted research on velocity cap using Flow-3D. They stated the $k-\epsilon$ model has the best performance among turbulent models. Chie and Wahab (2020) studied the design criteria of the octagonal shape of the velocity cap by Flow-3D model. They stated that the intake opening ratio (Or) should be $0.36 Vr - 0.31$, where $Vr = Vo/V_{pipe}$ (Vo is the velocity at the intake window and V_{pipe} is the suction velocity at the intake pipe). Sufficient, constant, uniform flow as well as high quality water shall be considered in designing the intake structure. The non-uniform influx and surface vortex reduce the efficiency of intakes and coastal facilities considerably. The main use of the velocity cap is to create a smooth flow around entrances, prevent environmental effects on intake, and protect the intake from the formation of a surface vortex. Firozjaei et al. (2023) stated caps play a significant role in removing the

surface vortex. They conducted research on the discharge coefficient of deep-water intake. As shown in Fig. 1, in the absence of velocity caps, the surface vortex is a great threat to the intake structure.

However, attention to bottom intake from reservoir and sea is increasing because of the unlimited water resources, the mechanism of velocity cap has not been evaluated clearly, which was mainly numerical. The lack of basic study on the effective parameters of velocity caps has been noticed. In this paper, the main parameters of velocity caps, such as shape, number of blades, and location of entrances, on discharge efficiency have been evaluated numerically and experimentally. Also, the flow pattern around the velocity caps is investigated based on an optic method using PIV (particle image velocimetry). In summary, the investigation presented in this study complements previous research, which predominantly utilized numerical methods, and offers valuable insights into the crucial aspects of bottom intake, with a specific focus on examining the velocity cap. Also, the research combines numerical modeling with experimental work to enhance the understanding of how velocity cap height and shape affect water intake. Combining experimental and numerical methods, a comprehensive analysis of the influential parameters on the discharge coefficient of bottom intake is presented. These analyses aim to provide valuable insights for hydraulic and marine engineers, guiding them in optimizing the design of bottom intake structures to improve the efficiency of water intake systems. It provides a comprehensive understanding of how these parameters influence the efficiency and overall performance of the intake process. The flowchart of this research is shown in Fig. 2. The presented investigation complements previous work and aims

Fig. 1 Surface vortices in a bottom intake without velocity cap



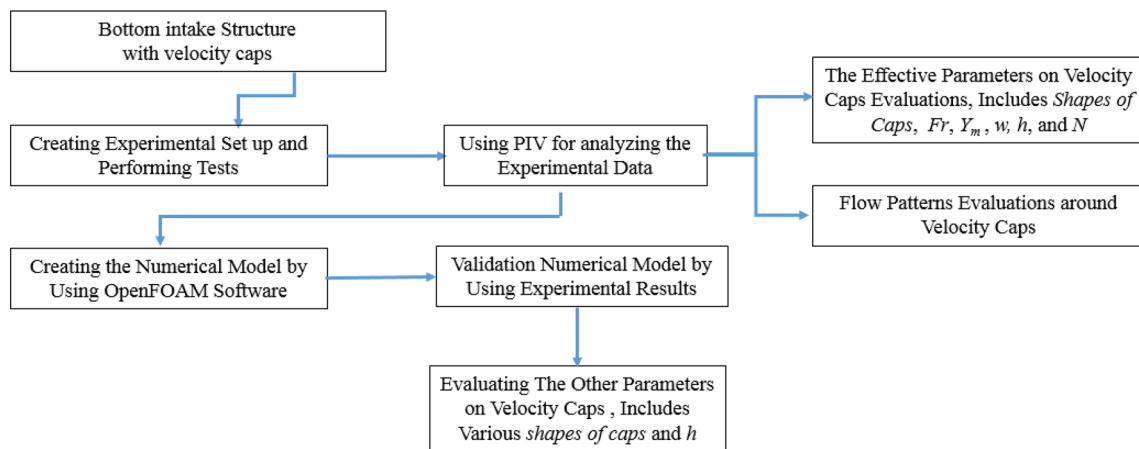


Fig. 2 Flowchart of the research method

to investigate the nature of the effective parameters for the discharge coefficient and flow pattern of the velocity cap structure.

Analytical considerations

The study of intake structures has a long history, and it is considered one of the most important types of hydraulic structures used to divert a portion of the flow. The same ideas can be considered for bottom intake structures, since few studies have been performed on such structures. The principle of energy for incompressible flows is expressed by Bernoulli’s equation. This balance ensures the continuity of the flow. Finally, by considering the losses of the whole system, which contain friction losses, minor losses, entrance losses, bend losses, and transition losses, the intake discharge is extracted as Eq. (1) (Hashid et al. 2015).

$$Q_{\text{intake}} = C_d \sqrt{2gH} \cdot \frac{\pi}{4} D^2 \tag{1}$$

Bottom intake is widely used to divert water from the sea, as a huge water reservoir, because of the lack of freshwater resources. Firozjaei et al. (2023) studied the discharge coefficient of seawater intake. They investigated the discharge coefficient of seawater intake. They stated that discharge through caps depends on Fr , w , h , Y_m , N , A , and the shape of the velocity caps. Where Fr is the Froude number on the main channel, Y_m is the water depth in the main channel, w is the distance of the opening of the intake from the channel bed, h is the height of the velocity cap, A is the area of the velocity cap, and N is the number of blades in velocity caps. This experimental and numerical study evaluates these factors in flow patterns around velocity caps and discharge through intake.

Experimental setup and procedures

The experimental setup, geometry of the caps, and the scaling rules applied in this study were already used in previous physical model tests by Firozjaei et al. (2023). Collected experimental parameters in this study are summarized in Table 1. In this study, 40 tests were conducted by using the full-factorial design method for both circle and square types. Recently, optical methods of flow imagination such as particle image velocimetry (PIV) are widely used in hydraulic researchers to measure fluid velocity. Small particles, which are supposed to follow flow faithfully, add to flow. Other techniques have been using to measure flows are acoustic doppler velocimetry (ADV) and current meter (Neogi et al. 2023). Also, it produces vector fields, while the other techniques measure the velocity at a point. Flow patterns have been extensively investigated by using flow visualizations in the fields of fluid dynamics, and hydraulic engineering. For detailed information about optical methods and details of the PIV algorithms, various investigations including Svizher and Cohen (2006), Meng et al. (2004), Baker et al. (2016), and Baker et al. (2016) can be reviewed.

Table 1 Overview of the datasets used in present study

Parameter	Unit	Range of data	
		Minimum	Maximum
Q	m^3/s	0.00357	0.00552
h	m	0.08	0.016
w	m	0.08	0.016
Y_m	m	0.26	0.36
V	m/s	0.0319	0.0383
Fr	Dimensionless	0.0178	0.0223
A	m^2	0.020	

Figure 3 shows the details of optic system. Typical optical sets contain camera, laser, and seeded flow. Particle characteristics, such as size and density, should be chosen to host no effect on flow (Webster et al. 2003). In this study, the camera used has a CMOS sensor and the ability to record pictures with a resolution of 800*600 pixels at the rate of 200 frames per second. Also, a continuous laser with an output power of 150 mw and a wavelength of 532 nm has been used.

Numerical model

Computational fluid dynamics has been recognized as a dependable approach for investigating hydraulic issues due to its cost-effectiveness and efficiency in terms of time. Its appeal lies in its ability to offer a cost-efficient and time-saving alternative for exploring and understanding various hydraulic problems (Badfar et al. 2021). OpenFOAM (open field operation and manipulation) is free, open-source powerful computing software that has an extensive range of features to solve anything, including complex fluid flows and turbulence. Until today, many studies have been carried out regarding fluid flows using OpenFOAM. Valela et al. (2021) investigated scouring around the bridge piers by OpenFOAM. For more detail on OpenFOAM, various references can be referred to, such as Yin et al. (2021). Christensen et al. (2014) studied the hydraulic performance of a velocity cap structure. They studied the circle shape of the velocity cap with different blades by using OpenFOAM. They used K- ω SST as a turbulent model. They observed the separation area on

the lee side of the velocity cap, which is dependent on current speed in the main channel. In this study, K- ω SST was applied as a turbulent model based on Christensen et al. (2014) and Doni (2018) who studied velocity caps using OpenFOAM. For detailed information about turbulent models and to study the K- ω SST method further, Mehranfar and Ghanbari-Adivi (2022) can be reviewed.

Flow equations

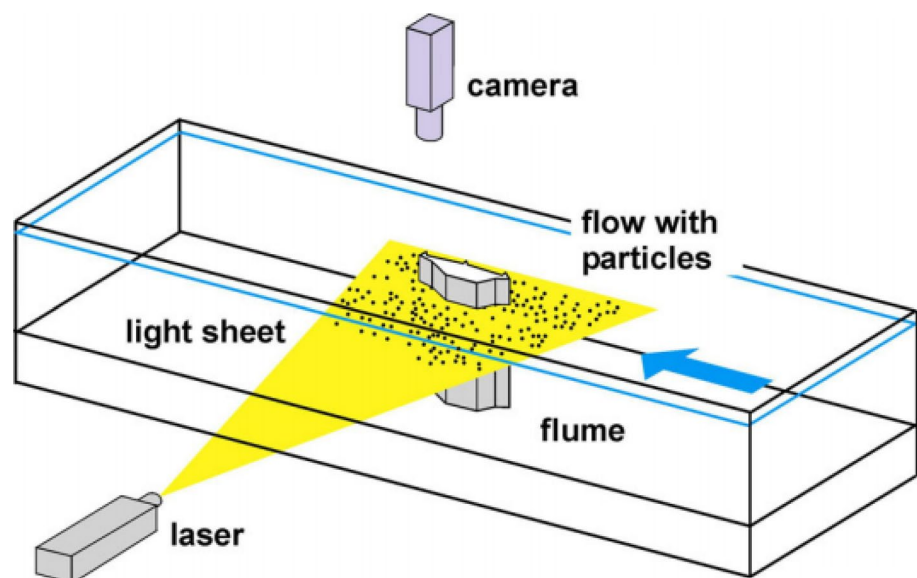
The volume of fluid method is a dependable approach for monitoring the air–water interface, offering various options to accurately reconstruct the interface while maintaining the fractional volume of fluid. However, VOF becomes challenging when calculating the curvature of the interface or other continuous properties is necessary. For details on how this method operates, refer to Shahheydari et al. (2015) and Heidarian et al. (2022). In this study, an InterFoam solver was used for modeling. The governing equations of free surface incompressible turbulent flow and viscous fluid that are known as RANS equations, are expressed as follows (Christensen et al. 2014):

$$\frac{\partial \rho}{\partial t} + \frac{\partial U_i}{\partial x_i} = 0 \quad (2)$$

$$\frac{\partial U_i}{\partial t} + U_i \frac{\partial U_i}{\partial x_j} = -\frac{1}{\rho} \frac{\partial p}{\partial x_i} + \frac{\partial}{\partial x_i} \left((\nu + \nu_t) \left(\frac{\partial U_i}{\partial x_j} + \frac{\partial U_j}{\partial x_i} \right) \right) \quad (3)$$

where U_i is the time averaged velocity in the i th direction, ρ is fluid density, ν is kinematic viscosity, and ν_t is the eddy viscosity, respectively.

Fig. 3 Schematic of the main components of a typical optic setup



Boundary conditions

The outcomes of numerical methods are significantly influenced by the imposition of boundary conditions. The proper specification of boundary conditions holds crucial importance in determining the accuracy and reliability of numerical simulations. The way boundary conditions are defined plays a pivotal role in shaping the results and ensuring the validity of the computational model Arami-Fadafan et al. (2018) and Barati et al. (2018). Following a thorough sensitivity analysis and a comprehensive review of the study conducted by Christensen et al. 2014, the selection of boundary conditions was approached with careful consideration, boundary conditions were selected as follows:

- Inlet: the inlet was considered as a fixed value velocity and zero gradient pressure. This permits the flow to enter symmetrically and flow freely into the channel.
- Outlets: a zero gradient pressure and a fixed value of velocity were considered for an outlet boundary of intake structures because it provides better control of the discharge.

- Atmosphere: pressure Inlet outlet velocity, here zero, and total pressure (uniform=0) were considered.

Validation of the numerical model

Experimental results are employed for the validation of the present numerical model. Following the generation of the geometry in OpenFOAM using SnappyHexMesh, a Cartesian-type grid is applied to the caps. The evaluation involved three sets of meshes with different grid numbers on the velocity caps. In order to check the accuracy of the number of meshes, the velocity magnitude around the circular cap was examined. Eventually, 1,300,000 meshes were selected. The comparison of experimental and numerical results of the velocity magnitude around the circular cap at the center line of the cap ($h/2$) is shown in Fig. 4. It can be seen that the numerical model can predict the formation of an area with maximum value with high accuracy. Also, the numerical model was evaluated by predicting the discharge through the velocity caps. Table 2 shows the comparison of numerical and experimental results. It can be seen that the numerical model has acceptable accuracy in predicting the discharge through the velocity caps. Also, the statistical

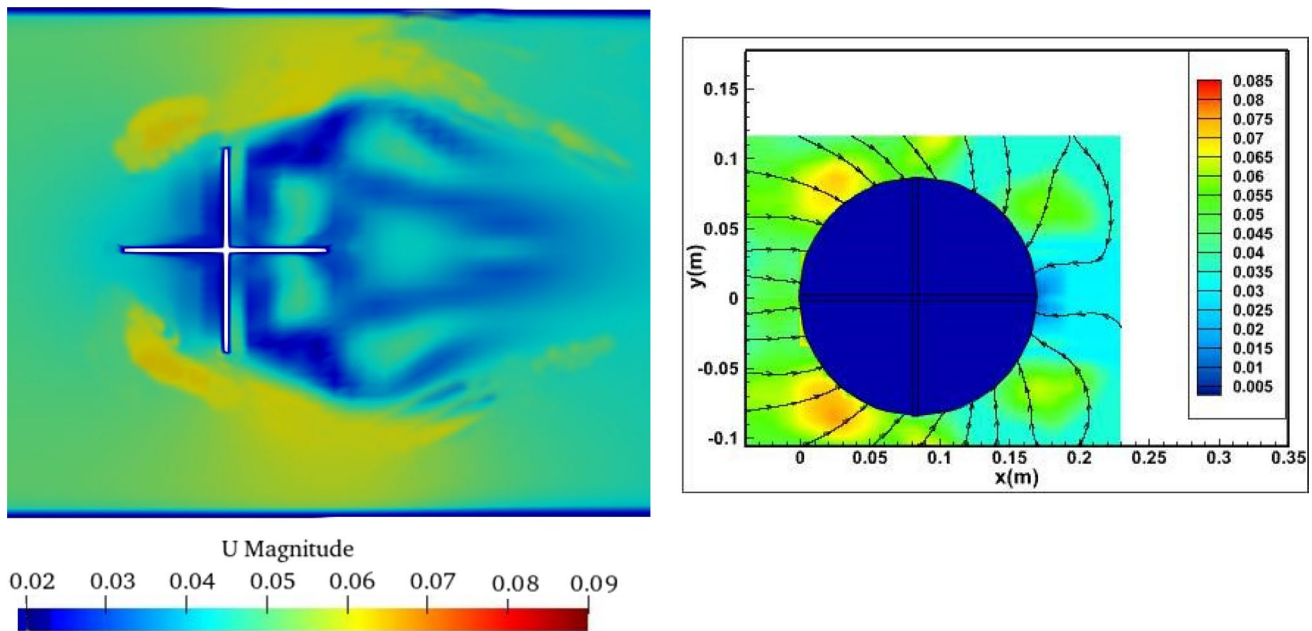


Fig. 4 Velocity magnitude validation using experimental data for the circular cap with $w=0.08$ m, $h=0.08$, and $N=4$

Table 2 Comparison of numerical and experimental results on flow rate

Run no.	Shape	Y_m (m)	w (m)	h (m)	N	Q_{intake} (m ³ /s)		Error (%)	RMSE
						Experimental	Numerical		
1	Circle	0.36	0.08	0.08	4	0.0055	0.0052	5.8	0.0003
2	Square	0.36	0.08	0.08	4	0.00518	0.0046	8.68	0.0006

index, root-mean-square error (RMSE), is employed to assess the precision and reliability of the numerical model.

$$RMSE = \sqrt{\frac{1}{n} \sum_{i=1}^N (X_p - X_m)^2} \tag{4}$$

Which n = the total number of data, X_p = predicted value, X_m = observed value.

Results

Observations during experiments

The formation of a surface vortex stands out as a major concern in bottom intake systems. Observations reveal a higher probability of surface vortex formation in square caps compared to circular caps (see Fig. 5). Additionally, it is observed that a surface vortex forms downstream of the velocity caps, significantly diminishing water intake efficiency. Consequently, in the context of vortex formation, circular caps demonstrate better performance than square ones. It's important to note that no experiments on velocity caps were conducted under these specific conditions.

Effect of the approach channel Froude number (Fr)

The effects of the approach channel Froude number on the C_d in different flow depth are shown in Fig. 6. It shows that C_d increases gradually by increasing the Fr , which is similar to the results of Hussain et al. (2010). Observations showed that Fr has a positive correlation with C_d , but the amount of its effect depends on other parameters, such as the geometric

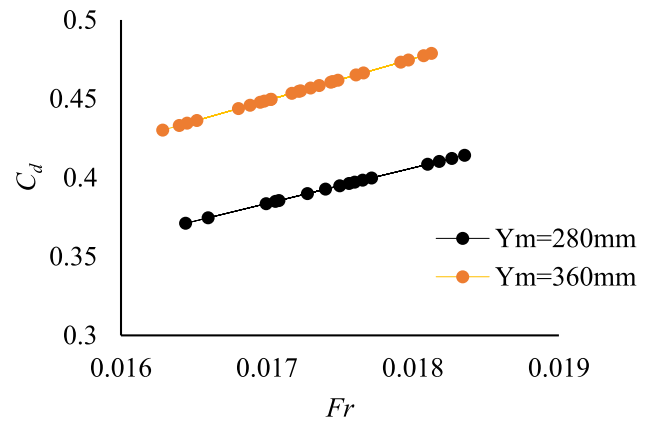


Fig. 6 Variation of C_d with Fr for velocity caps and different values of Y_m

parameter. This result is completely in agreement with the results of Firozjaei et al. (2023), who studied lateral pipe intake with various shaped entrances.

Effect of the flow depth (Y_m)

Observations show that there is a positive correlation between C_d and Y_m . This is because the seawater intake has more power for suction and power to go through the intake because the head of water above the centerline of the velocity caps increases. Figure 7 shows the velocity magnitude and streamlines for various flow depths. It can be defined that interactions between caps and flow are more tangible at low flow depth. It means that intakes feed from the area with a higher velocity, due to velocity distributions across the channel height. Consequently, turbulence increases. Streamlines show that the flow pattern around caps at higher depths

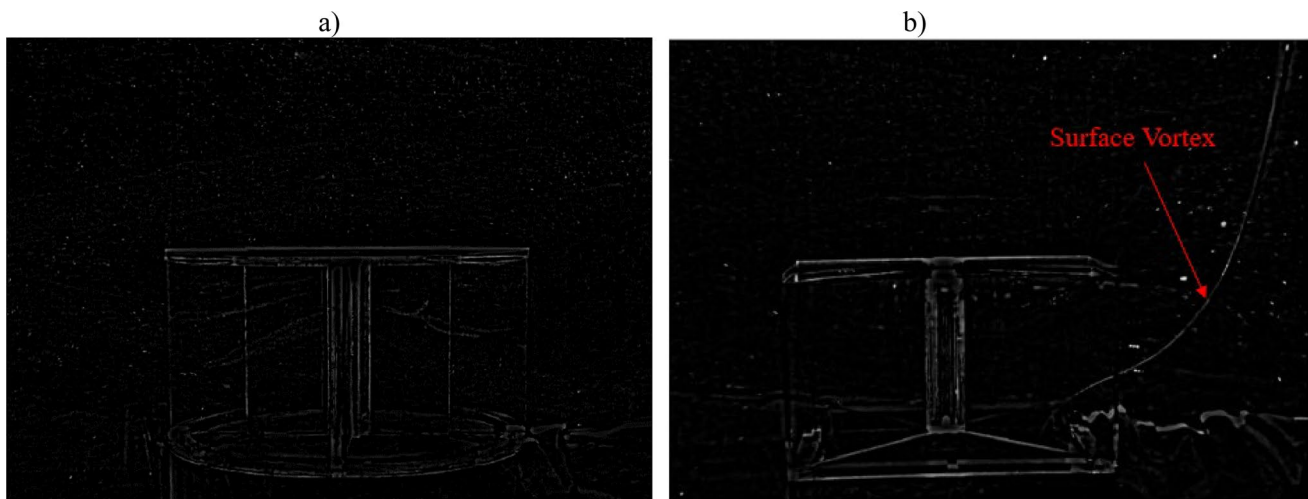


Fig. 5 Side view of formations of vortex in $Y_m = 260$ mm **a** circular velocity cap **b** square velocity cap

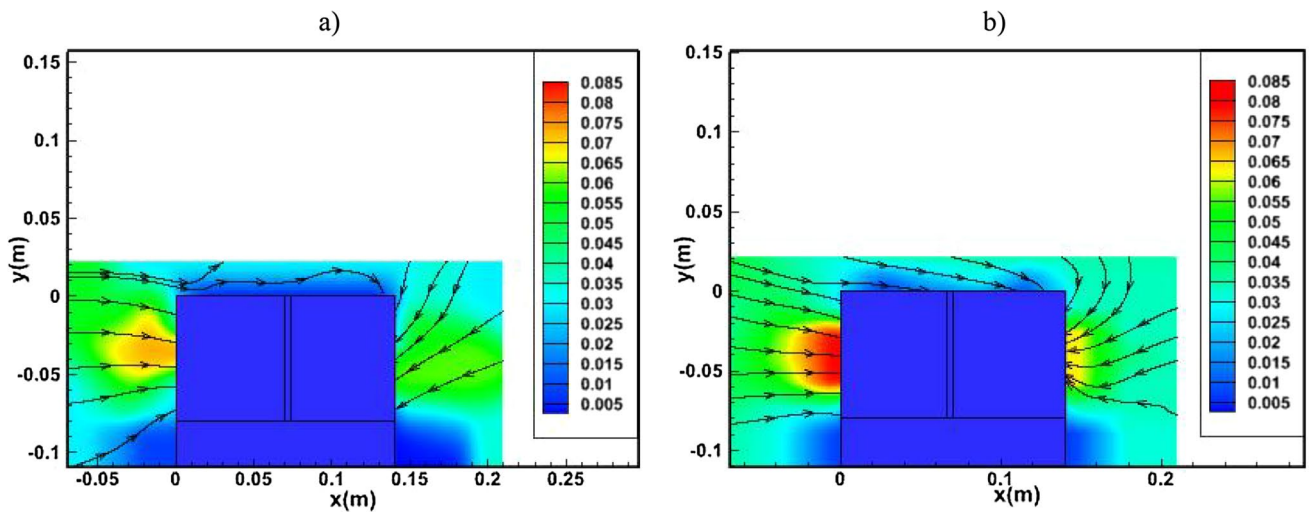


Fig. 7 Velocity magnitude and streamlines with $N=4$, $w=80$ mm, $h=80$ mm for square velocity cap a $Y_m=280$ mm b 360 mm

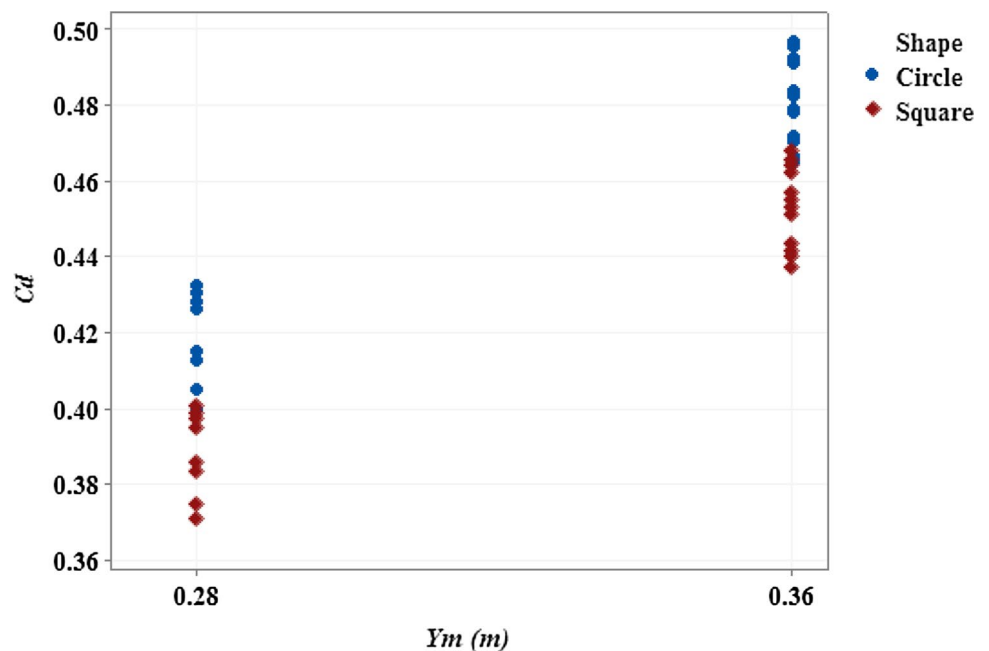
is smoother than at lower depths. As a result, the discharge through velocity caps increases.

Effect of velocity cap shapes

The most common type of velocity cap is a circle and square shape, which are evaluated in this study. Observations show that circle type has better performance than square type in terms of discharges through the intake. Results show that the discharge capacity of the circle velocity cap is a maximum of about 8% higher than that of the square cap. Figure 8 shows the variation between C_d and Y_m for two shapes.

In order to determine the role of the shape of the velocity cap, velocity magnitude contours and streamlines for circle and square types are shown in Fig. 9. As seen in Fig. 9, the streamline shows that flow could whirl in a more convenient path into the circle velocity cap rather than the square one. Also, it can be seen that a high velocity zone has formed in front of caps in square type, while it is located side of caps in circle caps. This can cause more friction force that should be considered in the design of the cap. Furthermore, the separation zone has formed at the back of velocity caps because of the complex behavior of diverted flow. This zone was more evident in square type; it is almost twice in the square case. Pervious investigations, such as Neary et al.

Fig. 8 Variation of C_d with Y_m for circle and square shapes



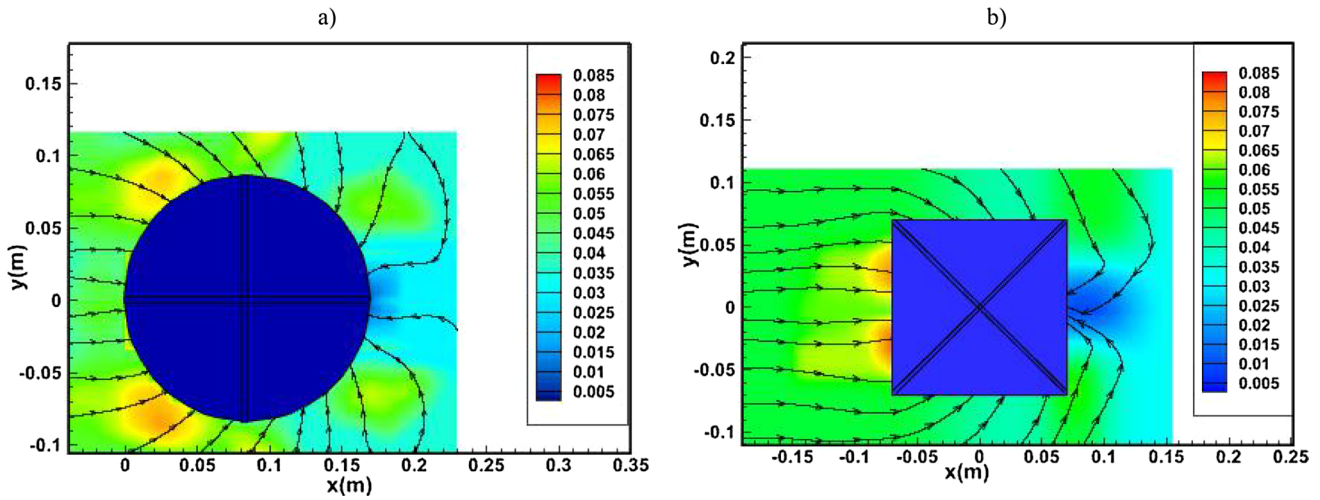


Fig. 9 Velocity magnitude contour and streamline in plan and side view **a** circle type **b** square type for $w=80$ mm, $h=80$ mm, $N=4$

(1999) and Barkdoll et al. (1999), have been conducted on lateral channel and pipe intake. Their result indicated that separation zones are created after the intersection with the lateral intake, near the sidewalls of the main channel. Observations of the bottom intakes indicate that the recirculation area locations in the main channel are completely different from a lateral open channel intake. It is similar to the lateral pipe intake.

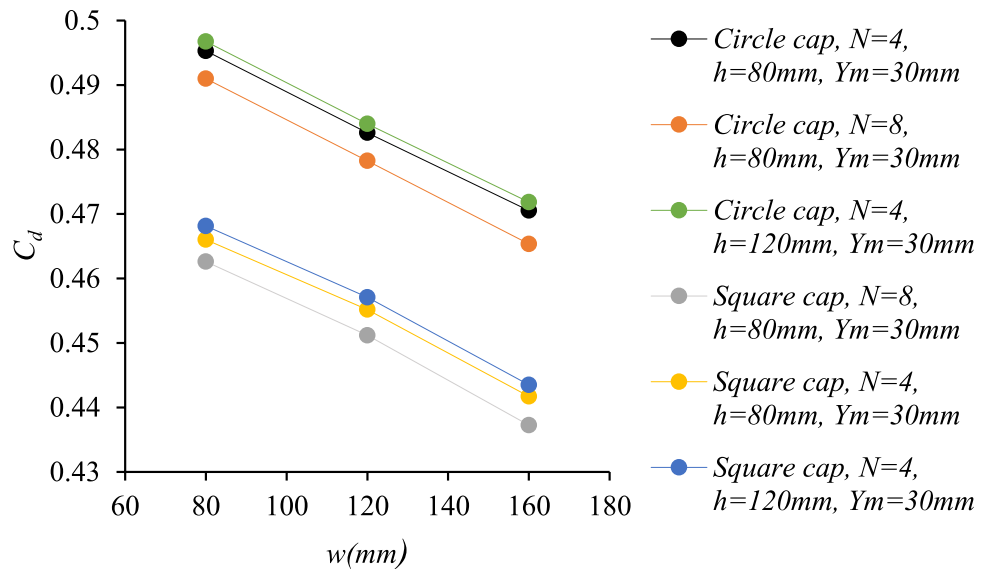
Effects of the velocity caps entrance location (w)

The variation between C_d and w is shown in Fig. 10. Observation shows that the distance of opening of intake from the channel bed (w) plays a reverse effect on C_d . This result is also observed for the side orifice, (Hussain et al. 2010).

This reverse performance happens because water intakes feed from the area with a lower velocity due to velocity distributions across the channel height.

In order to evaluate the velocity cap entrance locations, velocity magnitude contours and streamlines for three different w at the center line of circle velocity cap are shown in Fig. 11. As shown in the figure, by increasing w , the area of separation zones increases considerably, which intake discharge efficiency decreases. These observations were expected because the velocity cap structure works as an obstacle. Also, the streamline shows that water intake feeds from the area with a lower velocity due to velocity distributions across the channel height. Observations show that the swirling flow is formed at the top of the velocity cap and near the top of the cape, by increasing w . The streamline

Fig. 10 Variation of C_d with w for various parameters



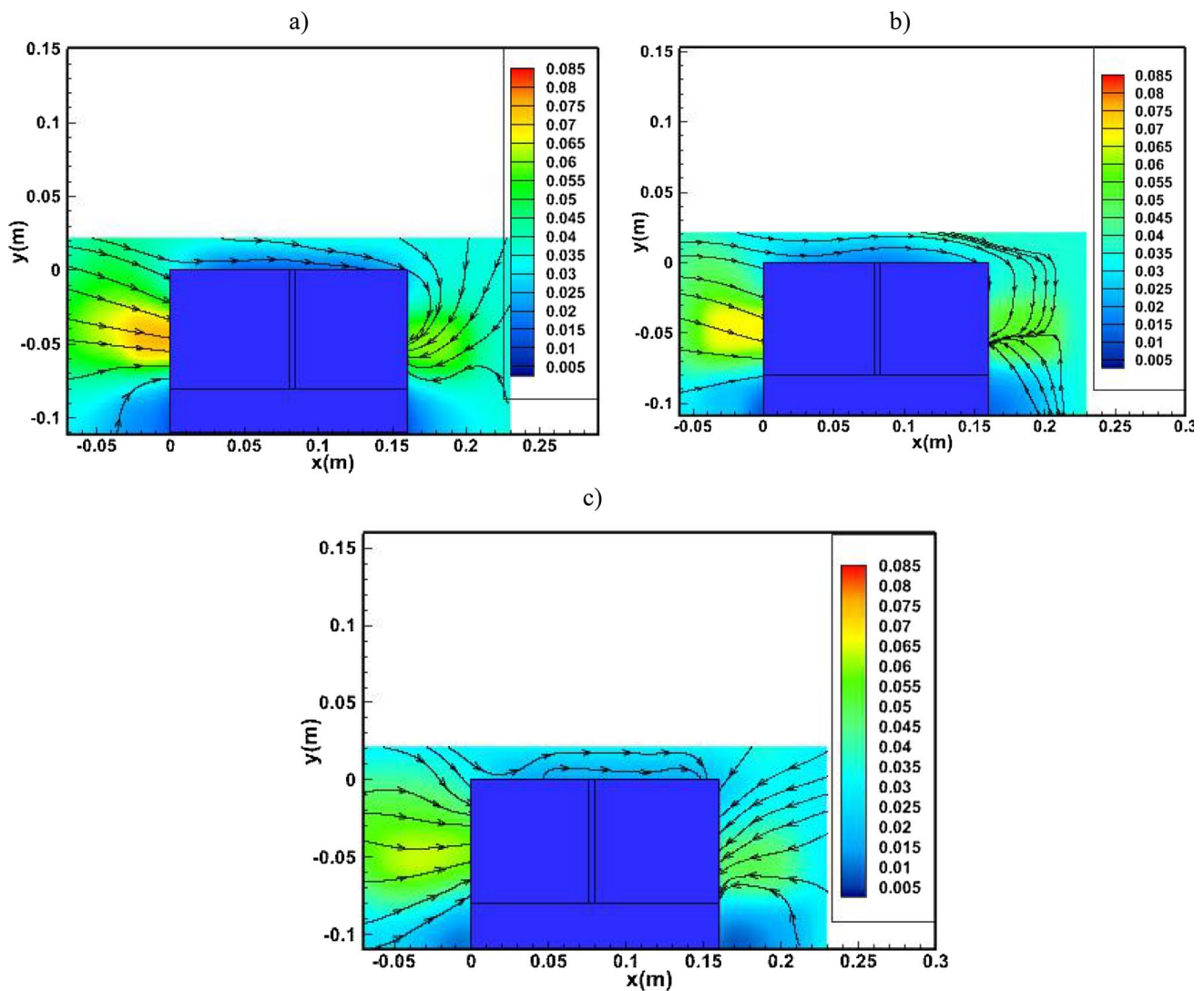


Fig. 11 Velocity magnitude contour and streamline at the centerline for $Y_m=360, h=80 \text{ mm}, N=4$ a $w=80 \text{ mm}$, b $w=120 \text{ mm}$ c $w=120 \text{ mm}$

shows that a convenient longitudinal flow pattern is formed around the velocity cap. Therefore, the lower height of the velocity cap entrance diverts larger discharges in comparison with other models.

Effect of velocity cap height (h)

Results show that from a certain point, the increase of h has not had much effect on the discharge efficiency. Figure 12 shows the velocity magnitude contours and streamlines at the center line of the circle velocity cap. Observations show that the complex flow is formed at the top of the backside of caps, by increasing h . This is because the flow is placed in a dilemma after hitting the wall of the velocity cap, so the recirculation flow pattern is formed. Based on the velocity magnitude contours, it is quite evident that the maximum current velocity happens near the entrances.

Effect of number of blades (N)

In order to control the overall flow pattern around velocity caps and smooth inlet flow, numerous blades are used in caps. As a result, injury and mortality of fish during downstream passage through seawater intake is significantly reduced. Correlation values indicate that C_d increases gradually by decreasing the number of blades. Moreover, according to the authors, the thickness of the blades can affect the percentage of their performance on the discharge efficacy. If the blade’s thickness increases considerably, it blocks and returns flow. So, it will have a negative impact on C_d . The effect of blade thickness can be investigated in future studies. Figure 13 shows the velocity magnitude contours and streamlines at the center line of the circle velocity cap. As can be seen, the flow pattern around caps in 8-blade caps is smoother than in 4-blade ones. This

result is completely similar to the results of Christensen et al. (2014).

Numerical simulation

After validating the numerical model, the effect of h was simulated with low values ($h = 0.04$ m). Results indicate that

by reducing the height of the caps by 50%, the intake efficiency decreases by 33% (see Table 3). Figure 14 shows the velocity magnitude for $h = 0.04$ m. As can be seen, the top of the caps prevents the current entrances. Flow hits the top of the cap and goes above it. Also, the discharge flow rate has been evaluated for the rhombus cap. Based on reported results in Table 3, by rotating 45° of the square caps (turning

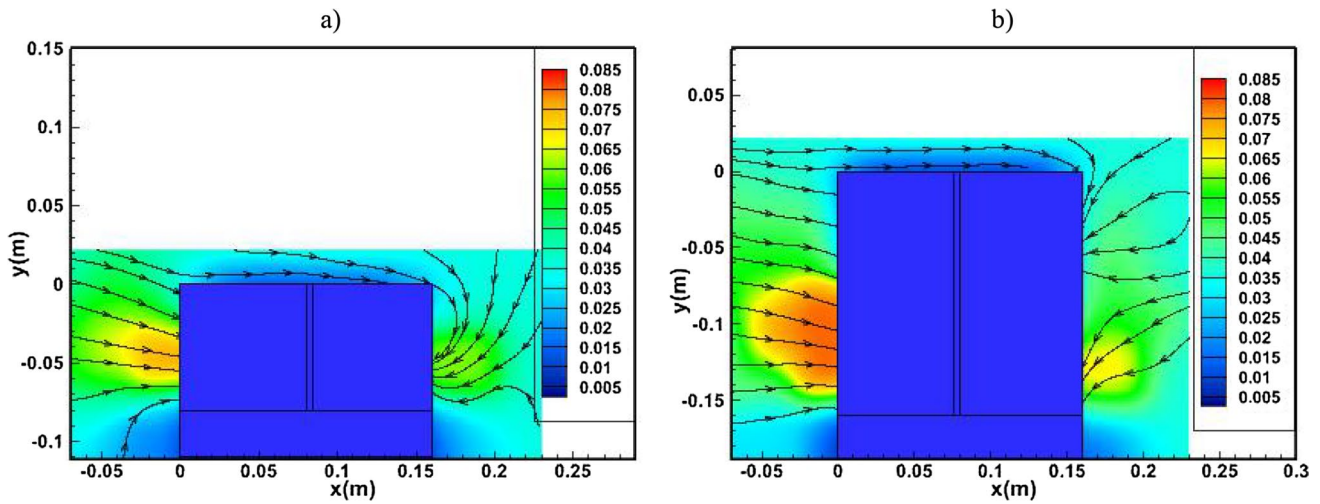


Fig. 12 Velocity magnitude contour and streamline at the centerline for $w = 80$ mm, $N = 4$ **a** $h = 80$ mm, **b** $h = 160$ mm

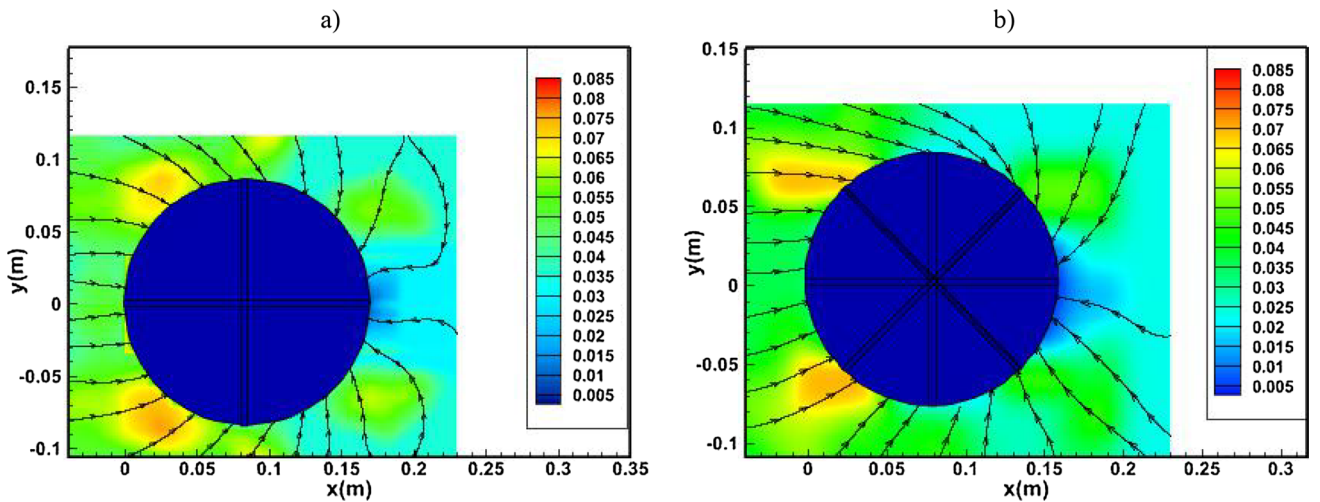


Fig. 13 Velocity magnitude contour and streamline at the centerline for $Y_m = 280$ mm, $w = 80$ mm, $h = 80$ mm, **a** $N = 4$ **b** $N = 8$

Table 3 Comparison of numerical results on flow rate for different parameters

Run no.	Shape	Y_m (m)	w (m)	h (m)	N	Q_{intake} (m^3/s)
1	Circle	0.36	0.08	0.08	4	0.0052
2		0.36	0.08	0.04	4	0.0035
3	Square	0.36	0.08	0.08	4	0.0046
4	Rhombus	0.36	0.08	0.08	4	0.005

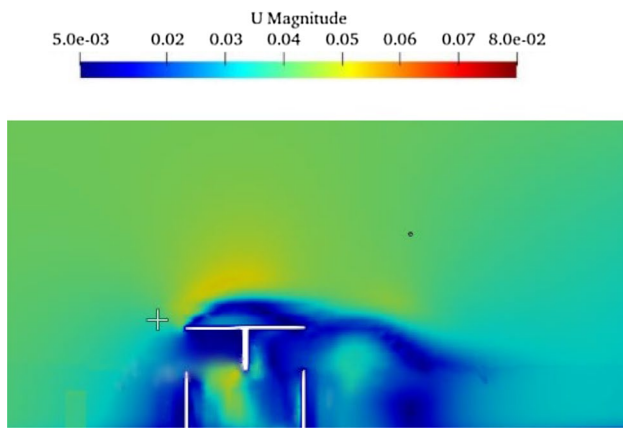


Fig. 14 Velocity magnitude contour at the centerline for $Y_m = 360$ mm, $w = 80$ mm, $h = 40$ mm, $N = 4$

into a rhombus cap in the flow direction), the discharge flow rate increases by about 7%.

Discussions

Water scarcity stands out as a pressing global social challenge, and regrettably, its prevalence is on the rise. The adoption of bottom intake systems is a prevalent practice to draw water from vast seawater reservoirs, particularly in regions facing a shortage of freshwater resources. Desalination technology emerges as a key solution embraced by humanity, notably in arid desert regions, exemplified by the countries surrounding the Persian Gulf. Typically, input water is delivered via deep water pipelines, and a potential environmental consequence arises from the elevated inflow velocity observed at intake sites. Consequently, velocity caps find widespread application at the intake header, serving the dual purpose of safeguarding marine life and ensuring the provision of the required flow rate. Additionally, these caps play a pivotal role in averting the formation of surface vortices, contributing to the overall environmental management of water intake systems. This experimental and numerical investigation builds upon earlier research, including but not limited to the works of Lee and Wahab (2019), Chie and Wahab (2020), and Christensen et al. (2014). The current study serves as a valuable addition to the existing body of research, enriching the understanding of the subject by incorporating insights from these prior studies.

During laboratory tests, it is natural to encounter uncertainties, which may include challenges in determining the appropriate method for calculating the flow rate. It is important to highlight that in this study, the comparison among various parameters was performed under constant conditions, resulting in minimal impact on the research outcomes.

An experimental investigation was conducted to explore the correlation between the parameters of flow depth, Froude number, entrance location, and velocity cap height concerning the water intake coefficient. This inquiry closely aligns with the results documented by Hussain et al. (2010), and Firozjaei et al. (2023), which were studied on lateral orifice and pipe intake. Also, the study integrates both numerical modeling and experimental efforts to advance the comprehension of how the height and shape of velocity caps influence water intake. This combined approach provides a synergistic perspective, leveraging the strengths of both numerical simulations and practical experiments to offer a more comprehensive understanding of the intricate dynamics associated with the impact of velocity cap characteristics on water intake systems. Through both experimental and numerical comparisons of three shapes (rhombus, square, and circle), it becomes evident that the circular type outperforms the other types concerning discharges through the intake. The findings consistently highlight the superior performance of the circular shape, emphasizing its effectiveness in optimizing the discharge process in both experimental and numerical analyses (see Table 3).

Conclusion

Due to water scarcity, the design of bottom intake systems on ocean beds has been assessed to provide water for coastal facilities, including desalination plants. This system consists of a velocity cap to protect aquatic organisms and facilitate the inlet flow, directing water to the side basin. The presented experimental and numerical study complements previous works and aims to investigate the nature of the effective parameters on the discharge coefficient of the cap structure. The obtained results are as follows:

- (1) Observations reveal a higher probability of surface vortex formation in square caps compared to circular ones. Additionally, it is noted that a surface vortex forms downstream of the velocity caps, significantly diminishing water intake efficiency. Consequently, in terms of vortex formation, circular caps exhibit superior performance compared to square ones.
- (2) Observations indicate that the circular type outperforms the square type in terms of discharges through the intake. Results demonstrate that the discharge capacity of the circular cap is approximately 8% higher than that of the square cap. This is attributed to the more convenient path for flow whirling into the circular caps compared to the square ones.
- (3) A separation zone has formed at the back of velocity caps due to the complex behavior of the diverted flow.

This zone is more prominent in the square type; it is almost twice in the square case.

- (4) The data illustrates a gradual increase in C_d with the rise in both Fr and Y_m . This is attributed to the increased power of bottom intake for suction and passage through the intake, driven by the heightened head of water above the centerline of the velocity caps. It appears that turbulence around the caps decreases with an increase in flow depth in the main channels, an aspect that permits more detailed exploration in future studies. In contrast, observations indicate that w exerts a reverse effect on C_d . This reverse performance arises from water intakes feeding from an area with lower velocity due to velocity distributions across the channel height.
- (5) Experimental and numerical results indicate that the velocity cap height (h) positively influences the discharge coefficient. The findings suggest that a 50% reduction in the height of the caps results in a significant 33% decrease in intake efficiency.
- (6) Numerical simulations on a rhombus cap (achieved by rotating the square cap by 45°) demonstrate an increase in discharge efficiency by approximately 7% compared to a square cap under the same conditions
- (7) In future studies, it is advisable to assess experimentally or numerically the discharge coefficient of the velocity cap under conditions involving cross-currents and surface waves. This approach would contribute valuable insights to further enhance our understanding of the performance of the velocity cap in diverse and dynamic marine environments.

Funding The author(s) received no specific funding for this work.

Declarations

Conflict of interest On behalf of all authors, the corresponding author states that there is no conflict of interest.

Ethical approval This essay doesn't have any ethical problems, and international standards regarding human and animal rights have been observed.

Open Access This article is licensed under a Creative Commons Attribution 4.0 International License, which permits use, sharing, adaptation, distribution and reproduction in any medium or format, as long as you give appropriate credit to the original author(s) and the source, provide a link to the Creative Commons licence, and indicate if changes were made. The images or other third party material in this article are included in the article's Creative Commons licence, unless indicated otherwise in a credit line to the material. If material is not included in the article's Creative Commons licence and your intended use is not permitted by statutory regulation or exceeds the permitted use, you will

need to obtain permission directly from the copyright holder. To view a copy of this licence, visit <http://creativecommons.org/licenses/by/4.0/>.

References

- Aghazadeh K, Attarnejad R (2020a) Improved desalination pipeline system utilizing the temperature difference under sub-atmospheric pressure. *Water Resour Manage* 34:1–19. <https://doi.org/10.1007/s11269-019-02415-4>
- Aghazadeh K, Attarnejad R (2020b) Study of sweetened seawater transportation by temperature difference. *Heliyon* 6(3):e03573. <https://doi.org/10.1016/j.heliyon.2020.e03573>
- Arami-Fadafan M, Hessami-Kermani MR, Barati R (2018) Applications of improved moving particle semi-implicit method for numerical simulation of flow over hydraulic structures. In: International energy and environment foundation, progress in river engineering & hydraulic structures, chapter four. 55–92
- Badfar M, Barati R, Dogan E, Tayfur G (2021) Reverse flood routing in rivers using linear and nonlinear Muskingum models. *J Hydrol Eng* 26(6):04021018. [https://doi.org/10.1061/\(ASCE\)HE.1943-5584.0002088](https://doi.org/10.1061/(ASCE)HE.1943-5584.0002088)
- Baker JL, Barker T, Gray JMNT (2016) A two-dimensional depth-averaged-rheology for dense granular avalanches. *J Fluid Mech* 787:367–395. <https://doi.org/10.1017/jfm.2015.684>
- Barati R, Neyshabouri SAAS, Ahmadi G (2018) Issues in Eulerian-Lagrangian modeling of sediment transport under saltation regime. *Int J Sedim Res* 33(4):441–461. <https://doi.org/10.1016/j.ijsrc.2018.04.003>
- Barkdoll BD, Ettema R, Odgaard AJ (1999) Sediment control at lateral diversions: limits and enhancements to vane use. *J Hydraul Eng* 125(8):862–870. [https://doi.org/10.1061/\(ASCE\)0733-9429\(1999\)125:8\(862\)](https://doi.org/10.1061/(ASCE)0733-9429(1999)125:8(862))
- Chie LH, Abd Wahab AK (2020) Derivation of engineering design criteria for flow field around intake structure: a numerical simulation study. *J Mar Sci Eng* 8(10):827. <https://doi.org/10.3390/jmse8100827>
- Christensen E, Eskesen M, Buhrkall J, Jensen B (2014) Analyses of hydraulic performance of velocity caps. In: 3rd International Association for Hydro-Environment Engineering and Research Europe Congress. <https://doi.org/10.1115/OMAE2015-41907>
- Doni G (2018) Force characterization for a submerged velocity cap in unsteady flows. Master thesis, University of Technology
- Firozjaei MR, Naeeni STO, Akbari H (2023) Evaluation of seawater intake discharge coefficient using laboratory experiments and machine learning techniques. *Ships Offshore Struct*. <https://doi.org/10.1080/17445302.2023.2247125>
- Greenlee LF, Lawler DF, Freeman BD, Marrot B, Moulin P (2009) Reverse osmosis desalination: water sources, technology, and today's challenges. *Water Res* 43(9):2317–2348. <https://doi.org/10.1016/j.watres.2009.03.010>
- Hashid M, Hussain A, Ahmad Z (2015) Discharge characteristics of lateral circular intakes in open channel flow. *Flow Meas Instrum* 46:87–92. <https://doi.org/10.1016/j.flowmeasinst.2015.10.005>
- Heidarian P, Neyshabouri SAAS, Khoshkonesh A, Bahmanpouri F, Nsom B, Eidi A (2022) Numerical study of flow characteristics and energy dissipation over the slotted roller bucket system. *Modeling Earth Syst Environ* 8(4):5337–5351. <https://doi.org/10.1007/s40808-022-01372-z>
- Hussain A, Ahmad Z, Asawa GL (2010) Discharge characteristics of sharp-crested circular side orifices in open channels. *Flow Meas Instrum* 21(3):418–424. <https://doi.org/10.1016/j.flowmeasinst.2010.06.005>

- Lee HC, Wahab AKA (2019) Performance of different turbulence models in predicting flow kinematics around an open offshore intake. *SN Appl Sci* 1:1–14. <https://doi.org/10.1007/s42452-019-1320-8>
- Mehranfar N, Ghanbari-Adivi E (2022) Numerical modeling of compound channels for determining kinetic energy and momentum correction coefficients using the OpenFOAM software. *Arch Hydro-Eng Environ Mech* 69(1):27–43. <https://doi.org/10.2478/heem-2022-0003>
- Meng H, Pan G, Pu Y, Woodward SH (2004) Holographic particle image velocimetry: from film to digital recording. *Meas Sci Technol* 15(4):673. <https://doi.org/10.1088/0957-0233/15/4/009>
- Missimer TM, Ghaffour N, Dehwah AH, Rachman R, Maliva RG, Amy G (2013) Subsurface intakes for seawater reverse osmosis facilities: capacity limitation, water quality improvement, and economics. *Desalination* 322:37–51. <https://doi.org/10.1016/j.desal.2013.04.021>
- Neary VS, Sotiropoulos F, Odgaard AJ (1999) Three-dimensional numerical model of lateral-intake inflows. *J Hydraul Eng* 125(2):126–140. [https://doi.org/10.1061/\(ASCE\)0733-9429\(1999\)125:2\(126\)](https://doi.org/10.1061/(ASCE)0733-9429(1999)125:2(126))
- Neogi A, Mohanta HK, Sande PC (2023) Particle image velocimetry investigations on multiphase flow in fluidized beds: a review. *Flow Measur Instrum*. <https://doi.org/10.1016/j.flowmeasinst.2023.102309>
- Shahheydari H, Nodoshan EJ, Barati R, Moghadam MA (2015) Discharge coefficient and energy dissipation over stepped spillway under skimming flow regime. *KSCE J Civ Eng* 19:1174–1182. <https://doi.org/10.1007/s12205-013-0749-3>
- Svizher A, Cohen J (2006) Holographic particle image velocimetry system for measurements of hairpin vortices in air channel flow. *Exp Fluids* 40(5):708–722. <https://doi.org/10.1007/s00348-006-0108-y>
- Valela C (2021) Reduction of bridge pier scour through the use of a novel collar design. Doctoral dissertation, Université d'Ottawa/University of Ottawa
- Webster DR, Rahman S, Dasi LP (2003) Laser-induced fluorescence measurements of a turbulent plume. *J Eng Mech* 129(10):1130–1137. [https://doi.org/10.1061/\(ASCE\)0733-9399\(2003\)129:10\(1130\)](https://doi.org/10.1061/(ASCE)0733-9399(2003)129:10(1130))
- Yin M, Zhao X, Luo M, Sun H (2021) Flow pattern and hydrodynamic parameters of pile breakwater under solitary wave using OpenFOAM. *Ocean Eng*. <https://doi.org/10.1016/j.oceaneng.2021.109381>

Publisher's note Springer Nature remains neutral with regard to jurisdictional claims in published maps and institutional affiliations.